



On the use of depth camera for 3D phenotyping of entire plants

Yann Chéné^a, David Rousseau^{b,*}, Philippe Lucidarme^a, Jessica Bertheloot^c, Valérie Caffier^c,
Philippe Morel^c, Étienne Belin^a, François Chapeau-Blondeau^a

^a Laboratoire d'Ingénierie des Systèmes Automatisés (LISA), Université d'Angers, 62 avenue Notre Dame du Lac, 49000 Angers, France

^b Université de Lyon, Laboratoire CREATIS; CNRS UMR 5220; INSERM U630; Université Lyon 1; INSA-Lyon, 69621 Villeurbanne, France

^c INRA, 42 rue Georges Morel boulevard, 49071 Beaucozoué, France

ARTICLE INFO

Article history:

Received 20 September 2011

Received in revised form 4 December 2011

Accepted 21 December 2011

Keywords:

Depth camera

3D measurements

Plants

High-throughput phenotyping

ABSTRACT

In this article, we assess the potential of depth imaging systems for 3D measurements in the context of plant phenotyping. We propose an original algorithm to segment depth images of plant from a single top-view. Various applications of biological interest involving for illustration rosebush, yucca and apple tree are then presented to demonstrate the practical interest of such imaging systems. In addition, the depth camera used here is very low cost and low weight. The present results therefore open interesting perspectives in the direction of high-throughput phenotyping in controlled environment or in field conditions.

© 2012 Elsevier B.V. All rights reserved.

1. Introduction

A current bottleneck in biology is the development of automated measurement methods to study phenotypic traits. This opens challenges in the domain of sensors (Ruiz-Altisent et al., 2010), information processing (Haff et al., 2010) or data compression (Belin et al., 2011). In this framework, computer vision tools offer a large panel of noninvasive techniques. In this report, we demonstrate the potential and interest of low cost depth cameras for various 3D measurements attached to architecture or shape of plants.

Plant architecture is a trait of major interest in the domain of plant phenotyping. It is an essential variable in plant adaptation to environment (Evers et al., 2011) and can be used in plant breeding to define optimum varieties in different environments. In the case of ornamental plants, assessing external shape is also a key issue to control visual quality and commercial value (Boumaza et al., 2010). In research, plant architecture can bring important information to understand physiological processes governing plant functioning (Bertheloot et al., 2011a,b; Evers et al., 2011; Vos et al., 2010; Dornbusch et al., 2007). However, the development of efficient tools assessing entire plant architecture is still a major stake.

Nowadays, 3D laser scanners or X-ray tomographs make it possible to record a full 3D acquisition and reconstruction of entire

plants. 3D laser scanners can provide access to the branching and shoot structure (Van der Zande et al., 2006; de Mezzo et al., 2003; Cété et al., 2009; Binney and Sukhatme, 2009; Gorte and Pfeifer, 2004; Preuksakarn et al., 2010; Yan et al., 2009) while X-ray tomographs are specially well-adapted to trace the 3D structure of the root (Fang et al., 2009; Bidet et al., 1999). Such imaging systems provide access to quantitative morphological measurements that may be targeted beforehand or after the acquisition. However, when applied to large population of plants, complete 3D acquisitions can be time expensive for high-throughput phenotyping and will also produce huge amount of data. In some biological contexts full reconstruction of entire plants may not be necessary to characterize specific aspects of the morphology. This is the case, for example, when only information about the canopy structure is required (Biskup et al., 2007; Omasa et al., 2007; Hosoi and Omasa, 2007; Teng et al., 2009; Zhu et al., 2008). In such cases, relatively low cost imaging system producing smaller amount of data per plant can be useful. In this article, we follow this approach and present, with various practical demonstrations, the potential of a low-cost RGB-depth camera for 3D measurements of entire plants.

Depth cameras are active imaging systems which shine light onto the scene. The light reflected from the scene is used to build the depth image whether by measuring the time of flight between emission and reception or by measuring the deformation of the spatially structured lighting pattern (Chen et al., 2008). Depth camera can be associated with conventional RGB imaging system producing, after registration, a four components RGB-depth image.

* Corresponding author.

E-mail address: david.rousseau@univ-lyon1.fr (D. Rousseau).

URL: <http://www.istia.univ-angers.fr/LISA/PHENOTIC> (D. Rousseau).

The accessibility of such RGB-depth imaging systems has recently increased with the introduction of low-cost RGB-depth originally designed for videogames. This opens new possibilities for low cost embedded image processing vision machines (see, for instance, Stuckler et al., 2010; Gonzalez-Sanchez and Puig, 2011; Shotton et al., 2011). In this report, we propose to assess the interest of such a low-cost RGB-depth camera for 3D measurements on the shoot of entire plants.

2. Camera

There is a whole family of inexpensive depth cameras which have been recently introduced for computer vision and videogames applications (see Li et al., 2011, for a technical comparison). We used a Kinect Microsoft® RGB-depth camera with the drivers and depth calibration procedure proposed by Microsoft®. The Kinect produces depth images from the analysis of spatially

structured lighting pattern. The price of the camera, at the time of writing this manuscript, is low, within 100 euros, and some 40 times lower than the price of classical time of flight depth cameras. This Kinect system measures 29 cm by 7 cm by 7 cm for few hundred grams. It is composed of two CMOS cameras and an infrared (IR) light source. A first camera, equipped with a 400–800 nm bandpass filter, is dedicated to the RGB imaging. The second camera, equipped with a 850–1100 nm bandpass IR filter, provides the depth image. This system produces 640×480 pixels RGB-depth images coded with a 16 bits dynamic and acquired at a rate of 30 frames per second. This is a rather low spatial resolution by comparison with a standard RGB camera but we will show it is sufficient for several phenotypic traits. The depth range is [0.8 m, 3.5 m]. This is rather low compared to usual depth camera working on a time-of-flight principle. The depth resolution is typically of 10 mm. Again, this is a rather poor resolution if one is interested in small plants like *Arabidopsis*. We are going to show with larger

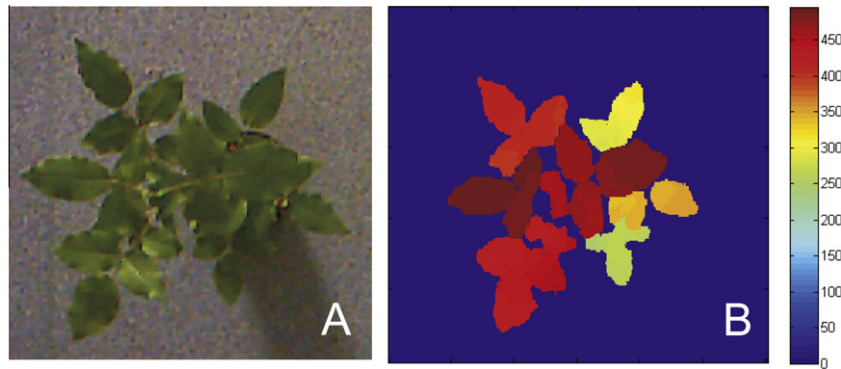


Fig. 1. (A) Top view RGB image of a rosebush. (B) Same rosebush as (A) with a depth camera scaled in mm with ground as reference.

```

% Algorithm Input–Outputs
Input: Depth image;
Output: Segmented image and Total number of objects;
% Geometric parameters
Minimum area = minimum area of a leaf;
Total depth = approximate plant height ;
Depth step = to be chosen smaller than the typical distance between leaves ;
% Algorithm parameter
Number of iterations = Round(Total depth / Depth step);

For i = 1 → Number of iterations
  Observed image = Depth image between [Maximum depth - i × Depth step, Maximum depth];
  Detection of n(i) Object, i.e. connected component, in Observed image;
  For j = 1 → n(i)
    If area of Object j ≥ Minimum area
      Storing spatial coordinates  $c_{i,j}(x, y)$  of Object j ;
      If  $i \geq 1$ 
        For k = 1 → n(i - 1)
          If  $c_{i,j}(x, y) = c_{i-1,k}(x, y)$ 
            Total number of object = Total number of object +1;
            Segmented image, pixels  $c_{i,j}(x, y) =$  Total number of object;
            Depth image, pixels  $c_{i,j}(x, y) = 0$ ;
          End If
        End For
      End If
    End For
  End For
End For

```

Fig. 2. Segmentation algorithm of leaves from depth image.

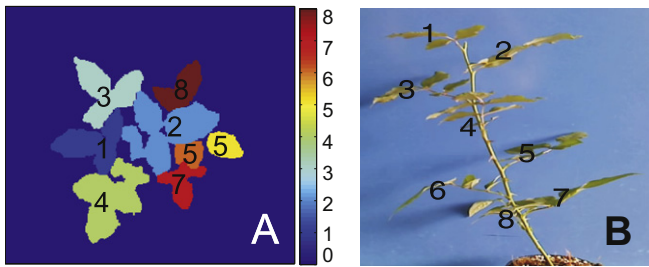


Fig. 3. (A) Leaves segmentation result for the rosebush of Fig. 1 with the algorithm of Fig. 2. Each color corresponds to an object identified as a separate segmented leaf. Numbers in (A) represent the order of appearance of each ground-truth leaf from the top of the plant to the ground. Numbers in (B) come from a direct visual inspection by a human expert from the side view of the rosebush. Ground-truth leaves 1, 2, 3, 4, 7 and 8 are correctly segmented. Ground-truth leaf 6, occluded by leaf 3, is not accessible from top-view. Ground-truth leaf 5, partially occluded by leaf 2 is segmented in two objects in the depth image. The height of the plant is approximately 0.5 m and the ground-truth leaves are clearly separated by more than the depth resolution 10 mm as requested by algorithm of Fig. 2. (For interpretation of the references to color in this figure legend, the reader is referred to the web version of this article.)

plants to which extent it can be useful for 3D measurement of shoot. The algorithm and applications presented below are in no way specific to the camera used for illustration in this report, but are relevant to depth camera in general. Motivations for the choice of the specific depth camera used in this report are its small size, low weight and low cost which make it suitable for in-field embedded phenotyping as well as high-throughput phenotyping when the system has to be replicated.

3. Leaves segmentation

A first important step in the 3D analysis of the shoot of plants is the segmentation of the leaves in images. We propose to tackle this segmentation task with a single top-view image acquisition. As visible in Fig. 1A, this is not an easy task with standard RGB images since leaves are usually poorly contrasted from one another and upper leaves may create shadow onto the lower leaves. The segmentation appears much easier from the depth image of Fig. 1B. To this purpose, we have developed and implemented the segmentation algorithm of Fig. 2. The principle is inspired from the maximally stable extremal regions algorithm introduced in computer vision for the segmentation of single object over background in gray level images (Matas et al., 2002; Mikolajczyk et al., 2005). The algorithm of Fig. 2 computes a scan in depth and detects an object to be segmented when a stable number of connected component is reached. Maximally stable extremal regions are therefore

Table 1

Angles measured with the depth camera between the two planes constituting the three leaves of the plant shown in Fig. 4.

Pair of vectors	Angle from camera in degree	Manual measure in degree
(\vec{u}_1, \vec{v}_1)	146 (± 2)	140 (± 3)
(\vec{u}_2, \vec{v}_2)	149 (± 2)	145 (± 3)
(\vec{u}_3, \vec{v}_3)	138 (± 2)	135 (± 3)

extended here to depth images and adapted to multiple object segmentation.

Some prior knowledge on the plant to be acquired is required as input to the algorithm of Fig. 2. These prior parameters are the plant height, the minimum expected area of a leaf, the depth step. The plant height can be obtained automatically if a colored landmark is placed on the ground. This landmark can be localized in the RGB image. The distance between the ground and the closest pixel captured in the depth image provides the size of the plant. The minimum expected area is assumed as biological prior and the minimum depth step is limited by the depth resolution of 10 mm. As a result of the constitution of algorithm of Fig. 2, any leaf captured by the depth image will be correctly segmented from the other leaves provided it is separated from the other leaves by a distance larger than the depth resolution of the camera. The algorithm of Fig. 2 has been tested for illustration on the rosebush of Fig. 1. Results are in good agreement with the ground truth. As visible in Fig. 3, this agreement holds when the leaf is visible from the top-view and when no partial occlusion divides the leaf into multiple objects in the depth image.

4. Applications

The segmentation of the leaves presented in the previous section opens access to any quantitative 3D measurements on the architecture of the shoot and structure of the segmented leaves of the plant. We provide some examples of application in this section.

As a first parameter, we demonstrate the possibility to measure leaf curvature with our depth camera. We considered for illustration here the ornamental plant (a yucca) of Fig. 4A where each leaf can be modeled as two connected planes with a definite angle. The angle between two vectors (\vec{u}, \vec{v}) of cartesian coordinates (X_u, Y_u, Z_u) and (X_v, Y_v, Z_v) is calculated as $\theta = \arccos(X_u X_v + Y_u Y_v + Z_u Z_v)$. As visible in Table 1, we measured this angle for various leaves from the depth image. These measures are simply made by selecting manually three points on the segmented image of Fig. 4B. Results are found in good agreement with a manual measurement while acquisition with the depth camera is much faster.



Fig. 4. (A) RGB image of the considered plant for leaf curvature measurement. (B) Depth image of the plant of (A). White arrows indicate the pairs of vectors (\vec{u}, \vec{v}) forming the two planes of the leaves. Angles between these vectors are given in Table 1.

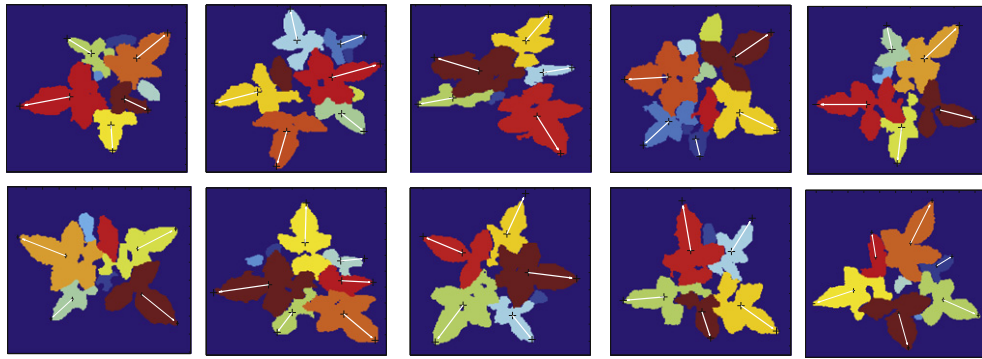


Fig. 5. Azimuth of the leaves for 10 rosebushes from depth camera. The automated measurement of the azimuth is materialized in solid white line.

Accuracy on the manual measure and on the depth image are estimated from multiple measurements on the same leaf. Manual accuracy is mainly limited by parallax or deformation of the leaves during the measurement. Angle measurements from depth images are limited by the depth resolution. The view in Fig. 4B is not a top-view of the plant as in the previous section. The choice of the camera position is not critical for the measurement but critically play on the visibility of the targeted elements of the plant to be measured.

When leaves are planar the curvature of the leaves may not be an interesting parameter. In such cases of plane leaves, another parameter to be estimated from top-view of segmented leaves is the orientation of the leaves. Leaf orientation on a plant determines plant capacity to intercept light for its photosynthesis and thus for its competitiveness to other species or varieties. The orientation of planar leaves can be assessed by the unit vector normal to the plane, defined by two angles: (1) the azimuth angle, i.e. the angle between the projection of the normal vector on a horizontal plane and the north; and (2) the zenith angle, i.e. the angle between the normal vector and the vertical. For illustration, we perform azimuth angle measurement from the segmented depth image. To this purpose, we calculate the coordinates of the inertial center and detect the extremity of the largest leaflet for each leaf. The azimuth direction can then be computed along those two points given

the north direction. The good quality of the results obtained for 10 rosebushes similar to the one of Fig. 3 can be appreciated from the visual inspection of Fig. 5. Such results could hardly be obtained from single top-view RGB image like Fig. 3 since there is almost no contrast to separate the leaves. For a quantitative assessment of the quality of the measured azimuth we have performed manual measurement of azimuth with a MicroScribe® G2 (Immersion Corporation, San José, CA, USA) point digitizer. For the 10 rosebushes tested, the single top-view depth image captures 68% of the leaves. The average of the absolute value of the error between the automated measurement and the manual measurement is of 5%.

In addition, it is possible to fuse the segmented depth image with other images of the same plant produced by other camera. It can be, for instance, an RGB camera but also other imaging systems. For illustration in this report we choose to register the depth camera with a thermal imaging system. Thermal imaging has recently received considerable attention in plant sciences because it can provide information on water content, stomatal aperture, or plant freezing. This technique has specifically been shown useful to monitor the development of pathogens (Cherle et al., 2007; Oerke et al., 2006). We use here thermal imaging to detect the presence of apple scab (see (Bowen et al., 2011) for a recent review on apple scab) on trees inoculated by the pathogen in controlled conditions. We have considered the apple tree of Fig. 6 where apple

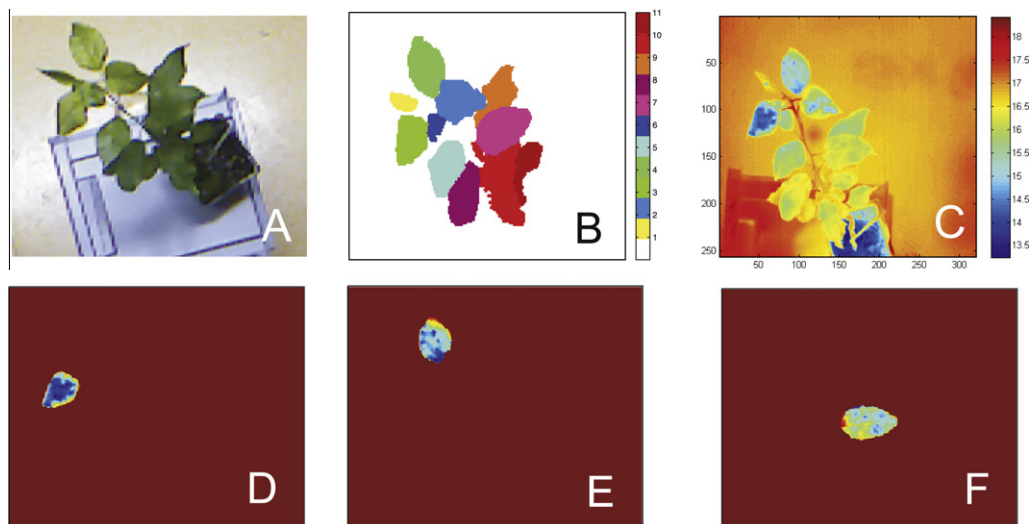


Fig. 6. (A–C) Registered images of the same apple tree, respectively stand for the RGB, thermal (scaled in degree Celsius) and segmented depth image. The apple tree presents apple scab pathogene on the three upper leaves. In (B) the scale is in integer. Each number corresponds to a segmented leaf. (D–F) The segmentation of the thermal image of (B) obtained from a binary multiplicative mask for three leaves of the apple tree of (A).

scab has been visually detected by an expert from a close-up inspection. At the scale of the entire plant, scab is not detectable with RGB imaging as shown in Fig. 6A, whereas scab is detectable with thermal imaging. This is visible in Fig. 6C where the three upper leaves show an apparent temperature with a 2 °C drop from other leaves. Leaves segmentation from thermal imaging can be difficult since ambient temperature can vary and some of the leaves can be poorly contrasted from the background. We therefore use the segmented depth image of Fig. 6B of the apple tree. Therefore, a simple multiplicative binary mask for each leaf is built and each binary mask is sequentially applied to select the thermogram of each leaf for scab detection on individual leaves. The entire apple tree can be scanned this way as depicted in Fig. 6D–F.

5. Conclusion and perspectives

We have demonstrated the possibility to use low-cost depth cameras for entire plant phenotyping with 3D measurements. We have proposed an original algorithm to segment the shoot of entire plants. Various biologically motivated applications from leaf curvature, leaf morphology, orientation or pathogen detection have been provided to establish the interest of depth camera for plant phenotyping.

Other applications could be undertaken like fruit volume estimation which could be performed in field. Also, in this report we have considered single top-views. It could be interesting to include side views and to study how depth images could be used to perform 3D full reconstruction. The algorithm introduced in this work does not require spatial information on the specific shape of the leaves or prior structural knowledge on the plants. Injecting such priors could be another interesting way for further investigations. The limitation of the proposed segmentation algorithm is attached to the depth resolution of the camera. Improving the depth improves the capability of the algorithm to segment smaller plants with more complex architecture and more compact shoot. Taking into account spatial prior information on the orientation of the leaves or their typical size or shape could be used to improve segmentation at fixed depth resolution. For instance, if one considers a plant which is known to present planar leaves, a binary classification test could be done on each pixel to decide if it belongs or not to the plane defined by a given leaf.

In the framework of phenotyping, plants are usually monitored one by one with noninvasive measurement tools. This is why we have, as a first proof of feasibility, dealt with single plants. However, an interesting strategy to increase the throughput is to acquire images under larger observation scales to capture multiple plants in one image. Also, in field conditions, the spatial arrangement of plants can be less regular than in perfectly controlled environment and multiple plants can be gathered in a single acquisition. This remains possible with the presently tested depth camera, as long as the set of plants fit in the field of view and depth range of [0.8 m, 3.5 m]. To deal with such multiple plant configuration, our segmentation strategy would have to include a separation step of the different plants. This could, for instance, be done by using the RGB components of our imaging system. For large plants, one would probably have to work in outdoor conditions with sunlight lightening. We have observed that strong IR radiations from sunlight can significantly degrade the measurements. In field conditions, acquisition with the depth camera used in this manuscript should thus have to be done at night or include a special modulation of the IR light of the depth camera to separate it from sunlight IR radiations.

Finally, depth cameras, like the one used in this report, usually shine an active IR component. This component is used to compute the depth image but it also carries information on the reflectivity of the leaves in the IR domain. These informations, not exploited here,

also constitute an interesting perspective for the use of depth-camera imaging for phenotyping.

Acknowledgments

This work is supported by la Région des Pays de la Loire, by le Conseil Général du Maine et Loire and by Angers Loire Métropole, in the framework of the collaborative project PHENOTIC.

References

- Belin, E., Rousseau, D., Léchappé, J., Langlois-Meurinne, M., Dürr, C., 2011. Rate-distortion tradeoff to optimize high-throughput phenotyping systems application to X-ray images of seeds. *Computers and Electronics in Agriculture* 77, 188–194.
- Bertheloot, J., Cournède, P.-H., Andrieu, B., 2011a. Nema, a functional-structural model of nitrogen economy within wheat culms after flowering. I: Model description. *Annals of Botany* 108 (6), 1085–1096.
- Bertheloot, J., Cournède, P.-H., Andrieu, B., 2011b. Nema, a functional-structural model of nitrogen economy within wheat culms after flowering. II: Evaluation and sensitivity analysis. *Annals of Botany* 108 (6), 1097–1109.
- Bidel, L., Mannino, M., Rivière, L., Pagès, L., 1999. Tracing root development using the soft X-ray radiographic method, as applied to young cuttings of western red cedar (*Thuja plicata*). *Canadian Journal of Botany* 77, 348–360.
- Binney, J., Sukhatme, G., 2009. 3D tree reconstruction from laser range data. In: *IEEE International Conference on Robotics and Automation (ICRA)*, pp. 1321–1326.
- Biskup, B., Scharr, H., Schurr, U., Rascher, U., 2007. A stereo imaging system for measuring structural parameters of plant canopies. *Plant, Cell and Environment* 30, 1299–1308.
- Boumaza, R., Huché-Théliér, L., Demotes-Mainard, S., Le Coz, E., Leduc, N., Pelleschi-Travier, S., Qannari, E., Sakr, S., Santagostini, P., Symoneaux, R., Guérin, V., 2010. Sensory profiles and preference analysis in ornamental horticulture: the case of the rosebush. *Food Quality and Preference* 21, 987–997.
- Bowen, J.K., Mesarich, C.H., Bus, V.G.M., Beresford, R.M., Plummer, K.M., Templeton, M.D., 2011. *Venturia inaequalis*: the causal agent of apple scab. *Molecular Plant Pathology* 12, 105–122.
- Cété, J., Widłowski, J., Fournier, R., Verstraete, M., 2009. The structural and radiative consistency of three-dimensional tree reconstructions from terrestrial lidar. *Remote Sensing of Environment* 113, 1067–1081.
- Chaerle, L., Leinonen, I., Jones, H.G., der Straeten, D.V., 2007. Monitoring and screening plant populations with combined thermal and chlorophyll fluorescence imaging. *Journal of Experimental Botany* 58, 773–784.
- Chen, S., Li, Y., Zhang, L., Wang, W., 2008. *Active Sensor Planning for Multiple View Vision Task*. Springer.
- de Mezzo, B., Fiorio, C., Rabatel, G., 2003. Weed leaves recognition in complex natural scenes by model-guided edge pairing. In: *4th European Conference on Precision Agriculture*. Berlin, Germany, pp. 141–147.
- Dornbusch, T., Wernecke, P., Diepenbrock, W., 2007. Description and visualization of graminaceous plants with an organ-based 3D architectural model, exemplified for spring barley (*Hordeum vulgare* L.). *The Visual Computer* 23, 569–581.
- Evers, J., van der Krol, A., Vos, J., Struijk, P., 2011. Understanding shoot branching by modelling form and function. *Trends in Plant Science* 16 (9), 464–473.
- Fang, S., Yan, X., Liao, H., 2009. 3D reconstruction and dynamic modeling of root architecture in situ and its application to crop phosphorus research. *The Plant Journal* 60, 1096–1108.
- Gonzalez-Sanchez, T., Puig, D., 2011. Real-time body gesture recognition using depth camera. *Electronics Letters* 53, 697–698.
- Gorte, B., Pfeifer, N., 2004. Structuring laser-scanned trees using 3d mathematical morphology. *International Archives of Photogrammetry and Remote Sensing* 35, 929–933.
- Li, L., Xu, Y., König, A., 2011. Robust depth camera based eye localization for human-machine interactions. *Lecture Notes in Computer Science* 6881, 424–435.
- Haff, R., Quinones, B., Swimley, M., Toyofuku, N., 2010. Automatic image analysis and spot classification for detection of pathogenic *Escherichia coli* on glass slide DNA microarrays. *Computers and Electronics in Agriculture* 71, 163–169.
- Hosoi, F., Omasa, K., 2007. Factors contributing to accuracy in the estimation of the woody canopy leaf area density profile using 3D portable lidar imaging. *Journal of Experimental Botany* 58, 3463–3473.
- Ruiz-Altisent, M., Ruiz-Garcia, L., Moreda, G.P., Renfu, L., Hernandez-Sanchez, N., Correa, E.C., Diezma, B., Nicola, B., Garca-Ramos, J., 2010. Sensors for product characterization and quality of specialty crops a review. *Computers and Electronics in Agriculture* 74, 176–194.
- Matas, J., Chum, O., Martin, U., Pajdla, T., 2002. Robust wide baseline stereo from maximally stable extremal regions. In: *British Machine Vision Conference*. Cardiff, UK, pp. 384–393.
- Mikolajczyk, K., Tuyelaars, T., Schmid, C., Zisserman, A., Matas, J., Schaffalitzky, F., Kadir, T., Van Gool, L., 2005. A comparison of affine region detectors. *International Journal of Computer Vision* 1, 43–72.

- Oerke, E.C., Steiner, U., Dehne, H.W., Lindenthal, M., 2006. Thermal imaging of cucumber leaves affected by downy mildew and environmental conditions. *Journal of Experimental Botany* 57, 2121–2132.
- Omasa, K., Hosoi, F., Konishi, A., 2007. 3D lidar imaging for detecting and understanding plant responses and canopy structure. *Journal of Experimental Botany* 58, 881–898.
- Preuksakarn, C., Boudon, F., Ferraro, P., Durand, J.-B., Nikinmaa, E., Godin, C., 2010. Reconstructing plant architecture from 3D laser scanner data. In: 6th International Workshop on Functional–Structural Plant Models, pp. 16–18.
- Shotton, J., Fitzgibbon, A., Cook, M., Sharp, T., Finocchio, M., Moore, R., Kipman, A., Blake, A., 2011. Real-time human pose recognition in parts from single depth images. In: IEEE Computer Vision and Pattern Recognition Conference. Colorado Springs, USA, pp. 1–7.
- Stuckler, J., Behnke, S., 2010. Combining depth and color cues for scale-and viewpoint-invariant object segmentation and recognition using random forests. In: International Conference on Intelligent Robots and Systems (IROS). Taipei, Taiwan, pp. 4566–4571.
- Teng, C., Kuo, Y., Chen, Y., 2009. Leaf segmentation, its 3D position estimation and leaf classification from a few images with very close viewpoints. *Image Analysis and Recognition* 5627, 937–946.
- Van der Zande, D., Hoet, W., Jonckheere, I., van Aardt, J., Coppin, P., 2006. Influence of measurement set-up of ground-based lidar for derivation of tree structure. *Agricultural and Forest Meteorology* 141, 147–160.
- Vos, J., Evers, J., Buck-Sorlin, G., Andrieu, B., Chelle, M., de Visser, P., 2010. Functional–structural plant modelling: a new versatile tool in crop science. *Journal of Experimental Botany* 61, 2101–2115.
- Yan, D., Wintz, J., Mourrain, B., Wang, W., Boudon, F., Godin, C., 2009. Efficient and robust reconstruction of botanical branching structure from laser scanned points. In: 11th IEEE International Conference on Computer-Aided Design and Computer Graphics (CAD/Graphics). Huangshan, China, pp. 572–575.
- Zhu, C., Zhang, X., Hu, B., Jaeger, M., 2008. Reconstruction of tree crown shape from scanned data. *Technologies for E-Learning and Digital Entertainment* 5093, 745–756.